Nuclear clustering using a modern shell model approach

Alexander Volya and Yury M. Tchuvil'sky

Phys. Rev. C **91**, 044319 — Published 20 April 2015

DOI: 10.1103/PhysRevC.91.044319

Study of nuclear clustering using the modern shell model approach

Alexander Volya[1] and Yury M. Tchuvil'sky[2]

[1]*Department of Physics, Florida State University, Tallahassee, FL 32306, USA*
[2]*Skobeltsyn Institute of Nuclear Physics, Lomonosov Moscow State University, 119991 Moscow, Russia*

(Dated: March 30, 2015)

Nuclear clustering, alpha decays, and multi-particle correlations are important components of nuclear dynamics. In this work we put forward the Cluster-Nucleon Configuration Interaction Model. We use the modern configuration-interaction approach with advanced realistic shell-model Hamiltonians in order to study clustering phenomena; the study is facilitated by the algebraic properties of many-nucleon configurations in the harmonic oscillator basis.

Using translationally invariant formalism we built cluster channels that satisfy Pauli exclusion principle as well as orthogonality and normalization conditions. We formally justify the formalism and demonstrate that, within the new method, clustering strengths satisfy sum rules that are consistent with the statistical properties of nuclear reactions with composite particles. Using properly renormalized cluster form factors our approach appears to resolve long-standing problems related to absolute normalization of the alpha clustering spectroscopic factors and their behavior in *sd*-shell nuclei.

Our methods are demonstrated in studies of α spectroscopic factors in *sd*-shell nuclei and in ^{16}O treated in *p*-*sd* shells. Comparison with experimental data supports validity of the approach.

PACS numbers: 21.60.Gx, 21.60.Cs

I. INTRODUCTION

Clustering, or an emergence of multi-nucleon substructures in a nucleus, is a pronounced and robust property of nuclear systems. The phenomenon is well confirmed experimentally: selective population of states in transfer and knock-out reactions, cluster decays, broad alpha-decaying resonances, features of electromagnetic form factors, as well as mass systematics – all support nuclear clustering. For an exhaustive overview we refer the reader to *Clusters in Nuclei* series [1]. Recent developments of experimental techniques such as inverse kinematics thick target technique [2, 3], have generated wealth of information concerning α-particle resonances in complex spectra, at high excitation energy, and for nuclei that manifest single-particle, collective, and cluster degrees of freedom [4–6].

A variety of theoretical techniques have been developed to study nuclear clustering, all approaching the problem from different directions, and with their specific advantages and disadvantages. Structure of highly clustered states have been explored using symmetry based approaches such as the one found in Ref. [7]; in this approach cluster degrees of freedom are introduced by construction. Within modern microscopic models such as the Antisymmetrized Molecular Dynamics [8] and Fermionic Molecular Dynamics [9], clustering properties of various nuclear states have been confirmed to emerge directly from nucleon-nucleon interactions. Cluster structures are seen in these models as peaks in the density distribution in the body-fixed coordinate frame; more quantitative techniques for evaluation of cluster and single-particle characteristics are yet to be developed. Other approaches stem from the microscopic *ab initio* direction; they include Green's Function Monte Carlo [10] and no-core shell model calculations of cluster reactions [11]. Computational complexity is the primary limitation of these *ab inito* calculations; this limitation renders studies of highly excited states infeasible at this time. In this presentation we turn to a configuration interaction approach which has the traditional nuclear shell model at its core. Our approach appears to be the middle ground among all techniques.

For over sixty years the nuclear shell-model approach has remained one of the most powerful theoretical tools available in studies of nuclear many-body problems [12–14]. The ability of the multi-configuration shell model (SM) to obtain level spectra and multiple other observables for a broad range of nuclear spectra using a single Hamiltonian, though be it somewhat phenomenological, gives this approach a practical advantage. Generalization in the form of the configuration interaction technique and applications involving the effective non-hermitian Hamiltonians permit treatment of weakly bound and unstable systems [15, 16]. Significant progress has been made towards *ab initio* understanding of the nucleon-nucleon interactions [17].

Advances in computational techniques and capabilities have broadened the areas of nuclear chart where shell model can be successfully applied. The small configuration space has always been the main criticism for this direction of work. With a few exceptions [18, 19], previous configuration interaction studies of clustering were limited to fixed-configurations or to paired, superfluid states [20, 21]. Modern, large-scale multi-configuration versions of the SM have prospect to overcome this criticism.

The study of cluster reactions and decays based on SM wave functions (WFs) has been continuously progressing [23–27] since the pioneering work [22]. Identification of quantitative measures of clustering characteristics

has been central in the development of clustering theory [22, 28]. The formalism for the description of clustering in the SM is presented in details in the monograph [29].

Let us emphasize the main ideas motivating further exploration and development of the shell-model approach to cluster physics.

First, over many years of research a large body of experimental data related to cluster physics in light- and medium-mass nuclei has been accumulated. As many as one hundred states and the corresponding alpha decay widths have been measured for certain isotopes. Recent experiments with resonance scattering of clusters, most commonly alpha-particles, have greatly benefited from the advent of thick target techniques in the inverse kinematics [2, 3]. These methods allow one to study dense spectra of cluster resonances in light (up to A $\sim$ 40) nuclei in wide energy ranges – see, for example, Refs.[4, 5, 30]. A good theoretical description of dense cluster spectra in a broad range of energies and a simultaneous description of other observables, such as single-nucleon emission, electromagnetic decays etc., remain difficult and out of reach for most theoretical techniques. Large scale shell model approach to clustering presented in this work provides some grip on this physics.

Second, the connection between the many-nucleon cluster channel WFs and the two-body cluster-nucleus optical model solutions has been brought to a better understanding in work [31], where the so-called "new spectroscopic factors" were proposed to meet the normalization and orthogonality conditions of the cluster channels. This definition represents a new mindset on the cluster processes and, while it eventually received broad support in the research community, see Refs. [32, 33], its application so far has been limited to alpha- and cluster radioactivity processes only. In the present work we accept this new definition, and promote it to the theory of direct and resonance nuclear reactions. We further contribute to the Fliessbasch's theory by developing an algebraic formalism of the new spectroscopic factors in the oscillator basis. Our studies support the validity of this approach and emphasize some important physical properties of the new spectroscopic factors.

Finally, advances in computational methods open a new era of nuclear structure theory. Shell-model calculations using extremely large-scale basis, such as in Ref. [34], have been very successful in reproducing and predicting the nuclear properties. This includes high excitation energy and high spin, single-particle and collective properties, electromagnetic and weak decays. *Ab initio* no core methods extend shell model toward the fundamentals of nucleon-nucleon physics [17, 35]. All of these advances are yet to be involved in the exploration of nuclear clustering.

In this work we present our approach, which is referred to as the Cluster-Nucleon Configuration Interaction Model (CNCIM). Some preliminary results, experimental studies, and examples not presented here can be found in [6, 36–39]. In the following sections we outline the formalism, and present two studies selecting deliberately simpler and more advanced limits that highlight the CNCIM. A brief summary is presented in Sec. IV.

II. FORMALISM

A. Fractional Parentage Coefficients in Configuration Interaction Approach

The single particle states are built using harmonic oscillator basis $\phi_{n\ell m}(\mathbf{r}) = \phi_{n\ell}(r)Y_{\ell m}(\Omega_{\mathbf{r}})$, the radial part being given by the function $\phi_{n\ell}(r)$; ℓ stands for orbital quantum number and m for its magnetic projection. We adopt a somewhat unusual notation by using n to denote the number of oscillator quanta, i.e., the main oscillator shell; this is different from the usual notation of the principal quantum number n, the number of nodes in the radial wave function, but the connection is simple: $n = 2n + \ell$. The angular part of the single particle wave function is given by the usual spherical harmonics $Y_{\ell m}(\Omega_{\mathbf{r}})$, which is then coupled with the spin part giving total angular momentum quantum number j and its magnetic projection m. An explicit form of the single particle wave functions for harmonic oscillator potential can be found in Ref. [40].

Following the strategy of the traditional shell model approach, the multi-nucleon wave functions are found as linear combinations of the Slater determinants of single particle states,

$$|\Psi\rangle \equiv \hat{\Psi}^{\dagger}|0\rangle = \sum_{\{1,2,3,\dots A\}} \langle 1,2\dots A|\Psi\rangle\, \hat{a}_1^{\dagger}\hat{a}_2^{\dagger}\dots\hat{a}_A^{\dagger}|0\rangle\,. \tag{1}$$

Here we use the formalism of the second quantization where $\hat{a}_1^{\dagger}$ represents the nucleon creation operator in the single particle state with the set of quantum numbers $1 \equiv \{n_1, \ell_1, j_1, m_1\}$. The numeric coefficient $\langle 1,2\dots A|\Psi\rangle$ in Eq. (1) determines the weight of each Slater determinant in the linear superposition. In Eq. (1) $|0\rangle$ denotes the vacuum state, and polymorphism between states and operators is highlighted by the introduction of the many-body creation operator $\hat{\Psi}^{\dagger}$.

The multi-nucleon states $|\{n_i^{\alpha_i}\}[f](\lambda,\mu)\colon L,S,T\rangle$ that carry the harmonic oscillator symmetry provide a basis for expansion of cluster channels. These states are identified by the configuration $\{n_i^{\alpha_i}\}$, where α_i denotes the number of particles in the major oscillator shell n_i. Therefore,

$$n = \sum_i \alpha_i n_i \quad \text{and} \quad A = \sum \alpha_i. \tag{2}$$

The symmetry is specified with the usual orbital, spin, and isospin quantum numbers, L, S, and T, respectively; (λ,μ) label the irreducible representation of Elliott's SU(3) group; and the Young frame specifies $[f]$ that classifies the permutation symmetry. In the present paper

we discuss alpha clustering, therefore we consider four-nucleon oscillator states with the permutation symmetry $[f]$=[4] characterized by the "stretched" SU(3) representation (λ,μ)=$(n,0)$

$$|\Phi^{\eta}_{(n,0):L}\rangle \equiv \Big(\hat{\Phi}^{\eta}_{(n,0):L}\Big)^{\dagger}|0\rangle \equiv \Big|\{n_i^{\alpha_i}\}[f]{=}[4](n,0)\colon L, S{=}0, T{=}0\Big\rangle. \quad (3)$$

The index η in the superscript identifies the configuration $\{n_i^{\alpha_i}\}$ and includes additional quantum numbers that may be necessary to uniquely distinguish the state from others. Strictly speaking, η is unnecessary for the particular cases considered in this work, since for the valence spaces considered, configurations are fully established by the total number of oscillator quanta, n. The states in Eq. (3) are constructed by diagonalization of linear combinations of second order Casimir operators; L^2, S^2, T^2 are used for orbital, spin, and isospin quantum numbers, and the SU(3) Casimir operator of the second rank is used to build a state that belongs to the irreducible representation $(\lambda{=}n,\mu{=}0)$; finally, the Majorana operator (sum of all possible pairwise permutation operators) is used to establish permutational and spin-isospin symmetry simultaneously.

The fractional parentage coefficient (FPC) between a parent state $|\Psi_P\rangle$ and an antisymmetrized product of an oscillator-symmetry state (3) and a daughter state $|\Psi_D\rangle$, where both parent and daughter states are of the form (1), is

$$\mathcal{F}^{\eta}_{nL} \equiv \langle\Psi_P|\hat{\mathcal{A}}\{\Phi^{\eta}_{(n,0):L}\,\Psi_D\}\rangle = \langle 0|\hat{\Psi}_P\{\hat{\Phi}^{\eta}_{(n,0):L}\hat{\Psi}_D\}^{\dagger}|0\rangle. \quad (4)$$

This is evaluated in the configuration interaction approach using the formalism of the second quantization where the antisymmetrization operator $\hat{\mathcal{A}}$ is inherent. The curly brackets in Eq. (4) imply a proper angular momentum coupling of the states $\Phi^{\eta}_{(n,0):L}$ and Ψ_D to that of the parent state Ψ_P; the magnetic quantum number is omitted for brevity of notations. The state-operator polymorphism facilitates manipulations with 4-nucleon states in Eq. (3). The FPCs for some selected states of SU(3) symmetry and related tests can be found in Ref. [39].

B. Traditional Cluster Spectroscopic Characteristics

The cluster form factor (CFF), also commonly referred to as the amplitude of the spectroscopic factor, is defined by the following expression

$$\varphi_{\ell}(\rho') = \Big\langle \hat{\mathcal{A}}\{\frac{\delta(\rho-\rho')}{\rho^2}\,Y_{\ell m}(\Omega_{\boldsymbol{\rho}})\Psi'_{\alpha}\,\Psi'_D\}\Big|\Psi'_P\Big\rangle, \quad (5)$$

where Ψ'_P, Ψ'_D, and Ψ'_{α} are internal, translationally invariant and free of the center of mass (c.m.) coordinate WFs of the parent (P) nucleus, the daughter (D) nucleus, and the α-cluster, respectively. The coordinate $\boldsymbol{\rho}$ is the Jacobi radial coordinate of the relative cluster-daughter motion, with ρ being its radial part. Here and in what follows we use primed notation to denote wave functions that have no dependence on the total center of mass (c.m.) variable of the system; one should distinguish these WFs from those of the shell model type (1). The relative cluster-daughter motion is considered separately for each partial wave ℓ, and a proper coupling to a relative angular momentum ℓ is established using spherical harmonics. As in Eq. (4), curly brackets imply that the angular momenta of daughter, alpha, and of their relative motion are coupled to the same value as the angular momentum of the parent system, thus the CFF does not depend on magnetic projection.

In connection with the harmonic oscillator basis discussed in Sec. II A it is convenient to expand the CFF using radial harmonic oscillator wave functions

$$\varphi_{\ell}(\rho) = \sum_n \langle\phi_{n\ell}|\varphi_{\ell}\rangle\,\phi_{n\ell}(\rho), \quad (6)$$

where the expansion coefficients $\langle\phi_{n\ell}|\varphi_{\ell}\rangle$ are known as spectroscopic amplitudes but, strictly speaking, represent the the fractional parentage coefficients of the translationally invariant shell model [41]

$$\langle\phi_{n\ell}|\varphi_{\ell}\rangle = \langle\hat{\mathcal{A}}\{\phi_{n\ell m}(\boldsymbol{\rho})\,\Psi'_{\alpha}\,\Psi'_D\}|\Psi'_P\rangle. \quad (7)$$

Next we describe a set of steps that allows one to obtain translationally invariant fractional parentage coefficients for an alpha particle in Eq. (7) from the fractional parentage coefficients for basis configurations (4) in non-translationally invariant SM formalism [23, 28, 29, 42]. Recent works in this direction can be found in Refs. [27, 43]. The many-body WFs Ψ_P and Ψ_D for the parent and the daughter systems are determined using the traditional SM approach. These WFs, in the form (1), depend on their c.m. coordinates R_P and R_D, respectively. In this work, as in a number of previous studies, the translational invariance of the SM wave functions is recovered by implementing the Glockner-Lawson procedure [40, 44]. This procedure results in a factorized form of the WF where the c.m. component is in the lowest oscillator state $\phi_{000}(\mathbf{R})$, namely,

$$\Psi_D = \phi_{000}(\mathbf{R}_D)\,\Psi'_D \;\text{ and }\; \Psi_P = \phi_{000}(\mathbf{R}_P)\,\Psi'_P. \quad (8)$$

The oscillator length parameter depends in the usual way on the mass number.

We assume that the intrinsic α-particle's WF Ψ'_{α} is represented by the lowest-energy translationally invariant four-nucleon configuration with quantum numbers $[f]$=[4], $(\lambda{=}0,\mu{=}0)$, and $L{=}S{=}T{=}0$. This wave function can be expressed using the shell model $(0s)^4$ configuration

$$|\Psi_{\alpha}\rangle \equiv \Big|(0s)^4[f]{=}[4](0,0) : L{=}0, S{=}0, T{=}0\Big\rangle, \quad (9)$$

where $\Psi_\alpha = \phi_{000}(\mathbf{R}_\alpha)\,\Psi'_\alpha$.

Let us now consider a general WF $\phi_{n\ell m}(\mathbf{R}_\alpha)\Psi'_\alpha$ where c.m. of the α-particle is in the harmonic oscillator state $\phi_{n\ell m}(\mathbf{R}_\alpha)$. Due to factorization (8) the following overlap

$$\langle \Psi_P|\hat{\mathcal{A}}\{\phi_{n\ell m}(\mathbf{R}_\alpha)\Psi'_\alpha\,\Psi_D\}\rangle = \langle \Psi'_P|\hat{\mathcal{A}}\{\phi_{n\ell m}(\boldsymbol{\rho})\Psi'_\alpha\,\Psi'_D\}\rangle \times \left\langle \phi_{000}(\mathbf{R}_P)\,\phi_{n\ell m}(\boldsymbol{\rho})|\phi_{n\ell m}(\mathbf{R}_\alpha)\,\phi_{000}(\mathbf{R}_D)\right\rangle \quad (10)$$

contains on the right-hand side a translationally invariant FPC (7) of interest. The second factor on the right-hand side appears due to the transformation from the c.m. coordinates of the daughter nucleus $\mathbf{R}_D$ and the cluster $\mathbf{R}_\alpha$ to the relative cluster – daughter motion described by coordinate ρ and the overall center-of-mass coordinate which coincides with $\mathbf{R}_P$:

$$\mathbf{R}_P = \frac{m_D\mathbf{R}_D + m_\alpha\mathbf{R}_\alpha}{m_D+m_\alpha}, \quad \boldsymbol{\rho} = \mathbf{R}_D - \mathbf{R}_\alpha. \quad (11)$$

The factor

$$\left\langle \phi_{000}(\mathbf{R}_P)\,\phi_{n\ell m}(\boldsymbol{\rho})|\phi_{n\ell m}(\mathbf{R}_\alpha)\,\phi_{000}(\mathbf{R}_D)\right\rangle \equiv \left\langle 00, n\ell:\ell|\{n\ell\}_{m_\alpha},\{00\}_{m_D}:\ell\right\rangle \quad (12)$$

is known as the oscillator bracket or Talmi-Moshinsky coefficient [45, 46]. For particles of different masses, as in the case here with daughter nucleus of mass m_D and alpha particle of mass m_α, the generalized oscillator bracket was studied by Smirnov [42, 47]; additional informative discussion and methods of evaluation can be found in Refs. [48, 49]. We define the recoil factor as the inverse of the oscillator bracket. Due to the simple Gaussian scalar form of the $0s$ oscillator state the recoil factor is given by an analytic expression that depends on the total number of the oscillator quanta n

$$\mathcal{R}_{n\ell} \equiv \left(\left\langle 00, n\ell:\ell|\{n\ell\}_{m_\alpha},\{00\}_{m_D}:\ell\right\rangle\right)^{-1} = (-1)^n\left(\frac{m_D+m_\alpha}{m_D}\right)^{n/2}. \quad (13)$$

Finally, the four-nucleon symmetry configurations (3) can be used as a basis for expansion

$$\phi_{n\ell m}(\mathbf{R}_\alpha)\Psi'_\alpha = \sum_\eta X^\eta_{n\ell}\,\Phi^\eta_{(n,0):\ell m}. \quad (14)$$

The expansion coefficients $X^\eta_{n\ell}$, referred to as the cluster coefficients, are known analytically [23, 28, 50],

$$X^\eta_{n\ell} \equiv \langle \Phi^\eta_{(n,0):\ell m}|\phi_{n\ell m}(\mathbf{R}_\alpha)\,\Psi'_\alpha\rangle = \sqrt{\frac{1}{4^n}\,\frac{n!}{\prod_i (n_i!)^{\alpha_i}}\,\frac{4!}{\prod_i \alpha_i!}}, \quad (15)$$

where n_i and α_i refer to the configuration of $\Phi^\eta_{(n,0):\ell}$, see Eqs. (3) and (2). Using expansion (14) in Eq. (10) we find a connection between the SM FPC $\mathcal{F}^\eta_{n\ell}$ in Eq. (4) and the translationally invariant FPC $\langle\phi_{n\ell}|\varphi_\ell\rangle$ for alpha particle in Eq. (7) in the following form [23, 28, 29, 42]:

$$\langle\phi_{n\ell}|\varphi_\ell\rangle = \mathcal{R}_{n\ell}\sum_\eta X^\eta_{n\ell}\,\mathcal{F}^\eta_{n\ell}\,. \quad (16)$$

C. New Cluster Spectroscopic Characteristics

It has been common in the literature to interpret the total norm of the CFF

$$\mathcal{S}^{(\mathrm{old})}_\ell = \langle\varphi_\ell|\varphi_\ell\rangle = \int \rho^2 d\rho\,|\varphi_\ell(\rho)|^2 = \sum_n |\langle\phi_{n\ell}|\varphi_\ell\rangle|^2 \quad (17)$$

as the spectroscopic factor. However, based on results in Ref. [51], Fliessbach argued in Refs. [31, 52] that the direct interpretation of $\varphi_\ell(\rho)$ as the the two-body cluster-nucleus solution is not appropriate. Let us discuss this next.

The cluster-nucleon motion is expressed using the channel WF

$$\Psi'_{\mathrm{ch}} = \hat{\mathcal{A}}\{f_\ell(\rho)Y_{\ell m}(\Omega_\rho)\Psi'_\alpha\,\Psi'_D\}. \quad (18)$$

The channel WF is subject to a many-body Schrödinger equation. It can be written in the form

$$\Psi'_{\mathrm{ch}} = \int f_\ell(\rho')\,\mathcal{P}_{\ell m}(\rho')\,\rho'^2 d\rho' \quad (19)$$

using a projector state $\mathcal{P}_{\ell m}(\rho')$ that depends on the parameter ρ',

$$\mathcal{P}_{\ell m}(\rho') \equiv \hat{\mathcal{A}}\{\frac{\delta(\rho-\rho')}{\rho^2}\,Y_{\ell m}(\Omega_{\boldsymbol{\rho}})\Psi'_\alpha\,\Psi'_D\}. \quad (20)$$

Projection of the many-body Schrödinger equation onto the radial degree of freedom using form (19) leads to the differential equation of the Resonating Group Method for one-dimensional WF $f_\ell(\rho)$,

$$\hat{\mathcal{H}}_\ell\,f_\ell(\rho) = E\hat{\mathcal{N}}_\ell f_\ell(\rho), \quad (21)$$

see Ref. [53] and references therein. This equation contains non-local linear operators $\hat{\mathcal{H}}_\ell$ and $\hat{\mathcal{N}}_\ell$ of integral type generated by the projection procedure

$$\langle\mathcal{P}_{\ell m}(\rho)|\Psi'_{\mathrm{ch}}\rangle = \hat{\mathcal{N}}_\ell f_\ell = \int \mathcal{N}_\ell(\rho',\rho)f_\ell(\rho)\rho^2 d\rho, \quad (22)$$

where the kernel is

$$\mathcal{N}_\ell(\rho',\rho'') = \langle \mathcal{P}_{\ell m}(\rho')|\mathcal{P}_{\ell m}(\rho'')\rangle = \Big\langle \hat{\mathcal{A}}\{\frac{\delta(\rho-\rho')}{\rho^2}Y_{\ell m}(\Omega_\rho)\Psi'_\alpha\,\Psi'_D\}\Big|\hat{\mathcal{A}}\{\frac{\delta(\rho-\rho'')}{\rho^2}Y_{\ell m}(\Omega_\rho)\Psi'_\alpha\,\Psi'_D\}\Big\rangle. \quad (23)$$

The kernel for $\hat{\mathcal{H}}_\ell$ is defined similarly using the microscopic Hamiltonian [54, 55]. The channel WFs are to be normalized in a usual way, namely, by Kronecker or Dirac delta functions for bound and continuum states, respectively. For brevity we use 1 to denote this normalization,

$$\langle \Psi'_{\rm ch}|\Psi'_{\rm ch}\rangle = \langle \hat{\mathcal{N}}_\ell^{1/2} f_\ell|\hat{\mathcal{N}}_\ell^{1/2} f_\ell\rangle = 1. \quad (24)$$

This shows that the function

$$F_\ell(\rho) \equiv \hat{\mathcal{N}}_\ell^{1/2} f_\ell(\rho), \quad (25)$$

and not the WF $f_\ell(\rho)$, is normalized to unity. Substituting $F_\ell(\rho)$ from Eq. (25) into Eq. (21) and acting with an operator $\hat{\mathcal{N}}^{-1/2}$ reduces this equation to the Orthogonality Conditions Model equation [51]

$$\hat{\mathcal{N}}_\ell^{-1/2}\hat{\mathcal{H}}_\ell\hat{\mathcal{N}}_\ell^{-1/2}F_\ell(\rho) = EF_\ell(\rho), \quad (26)$$

which has the form of an ordinary Schrödinger equation with a Hermitian effective Hamiltonian. Solutions of this equation corresponding to different eigenvalues are orthogonal. The norm operator $\hat{\mathcal{N}}$ is different from identity only for relatively small distances; therefore, $F_\ell(\rho)$ and $f_\ell(\rho)$ are equal in remote asymptotic regions, at $\rho\to\infty$. The asymptotic amplitude of these functions defines the intensities of observable channel flux and decay widths.

Establishing correspondence between the parent state Ψ'_P and the channel state $\Psi'_{\rm ch}$ is a central problem in studies of clustering. This correspondence can be established by comparison of projections where the multinucleon Hilbert space is projected onto the subspace of single coordinate ρ using (20). A key assumption of SM approach to the cluster problem is that the CFF $\varphi_\ell(\rho)$ obtained in the limited oscillator space extends far enough in separation distance permitting the comparison

$$\langle \mathcal{P}_{\ell m}(\rho)|\Psi'_P\rangle \equiv \varphi_\ell(\rho) \leftrightarrow \langle \mathcal{P}_{\ell m}(\rho)|\Psi'_{\rm ch}\rangle = \hat{\mathcal{N}}_\ell f_\ell(\rho). \quad (27)$$

While dealing with cluster channels one usually works with a solution of an ordinary two-body Schrödinger equation with Hermitian effective Hamiltonian which, obviously, possesses the normalization properties analogous to the ones of the function $F_\ell(\rho)$. Hence, the observed characteristics of resonance cluster scattering and cluster decay should be associated not with the traditional relationship $\varphi_\ell(\rho) \leftrightarrow F_\ell(\rho)$, but with the one of the form $\varphi_\ell(\rho) \leftrightarrow \hat{\mathcal{N}} f_\ell(\rho) = \hat{\mathcal{N}}^{1/2}F_\ell(\rho)$, see Eq. (27). Therefore, for $F_\ell(\rho)$ the correspondence $F_\ell(\rho) \leftrightarrow \psi_\ell(\rho)$ is established with a renormalized "new" cluster form factor

$$\psi_\ell(\rho) \equiv \hat{\mathcal{N}}_\ell^{-1/2}\varphi_\ell(\rho). \quad (28)$$

This leads to a new definition of the SF:

$$S_\ell^{(\rm new)} \equiv \langle\psi_\ell|\psi_\ell\rangle = \int \rho^2 d\rho\,|\psi_\ell(\rho)|^2\,. \quad (29)$$

It should be stressed that the SF is a definition-dependent theoretical concept and the proposed here definition is an attempt to best reflect the conventional choice of the channel wave function in the form of the solution of two-body Schrödinger equation.

The importance of this new definition is discussed in details in Refs. [21, 32]. We evaluate the redefined "new" cluster form factor using expansion in the oscillator basis. The matrix corresponding to the norm kernel in oscillator basis is

$$\langle\phi_{n'\ell}|\hat{\mathcal{N}}_\ell|\phi_{n\ell}\rangle = \langle\hat{\mathcal{A}}\{\phi_{n'\ell m}(\boldsymbol{\rho})\,\Psi'_\alpha\,\Psi'_D\}|\hat{\mathcal{A}}\{\phi_{n\ell m}(\boldsymbol{\rho})\,\Psi'_\alpha\,\Psi'_D\}\rangle. \quad (30)$$

The norm kernel matrix in the oscillator basis is evaluated using the second quantization techniques within the SM approach. Taking the steps similar to the ones described in Sec. II B, where in derivations it is convenient to use a complete set of intermediate parent states

$$\sum_P |\Psi_P\,\rangle\langle\,\Psi_P| \equiv \hat{1}\,, \quad (31)$$

one arrives at the following expression

$$\langle\phi_{n'\ell}|\hat{\mathcal{N}}_\ell|\phi_{n\ell}\rangle = \mathcal{R}_{n'\ell}\mathcal{R}_{n\ell}\sum_{\eta\eta'}X^{\eta'}_{n'\ell}X^{\eta}_{n\ell}\Big\langle 0\Big|\Big\{\hat{\Psi}^{\eta'}_{(n',0):\ell}\,\hat{\Psi}_D\Big\}\Big|\Big\{\hat{\Psi}^{\eta}_{(n,0):\ell}\,\hat{\Psi}_D\Big\}^\dagger|0\Big\rangle. \quad (32)$$

The coupling to particular channel quantum numbers that coincide with those of the parent nucleus is as-

sumed when curly brackets are used. In practical applications a matrix (32) for the norm operator is diagonalized, $\hat{\mathcal{N}}_\ell|k\ell\rangle = N_{k\ell}|k\ell\rangle$, here $|k\ell\rangle$ is an eigenvector and $N_{k\ell}$ is the associated eigenvalue, both corresponding to angular momentum ℓ. The expansion coefficients of the new CFF in the harmonic oscillator basis are

$$\langle\phi_{n\ell}|\psi_\ell\rangle = \sum_{k\,n'} \frac{1}{\sqrt{N_{k\ell}}}\langle\phi_{n\ell}|k\ell\rangle\langle k\ell|\phi_{n'\ell}\rangle\langle\phi_{n'\ell}|\varphi_\ell\rangle, \quad (33)$$

and the new SF is evaluated using an intermediate set of eigenstates of the norm operator and the harmonic oscillator basis as

$$S_\ell^{(\mathrm{new})} = \sum_k \frac{1}{N_{k\ell}} \left| \sum_n \langle k\ell|\phi_{n\ell}\rangle \, \langle\phi_{n\ell}|\varphi_\ell\rangle \right|^2 . \quad (34)$$

The new SFs are normalized; for any given parent nucleus the sum of all SFs for a given partial wave ℓ and to a particular daughter state equals to the number of doorway configurations (characterized by different values of n in four-nucleon functions $\Psi_{(n,0):l}$) involved. In order to demonstrate that, let us consider a complete set of parent states (31). For each state P we have a CFF in the form of a radial function $\varphi_\ell^{(P)}(\rho)$ defined by Eq. (5). The norm kernel can be calculated by including the complete set of parent states in Eq. (30). In the space of radial functions this means

$$\hat{\mathcal{N}}_\ell = \sum_P |\varphi_\ell^{(P)}\rangle\langle\varphi_\ell^{(P)}|. \quad (35)$$

By combining Eq. (35) and the definition in Eq. (29), and using an expansion in any radial basis states, one can show that the sum of SFs for all parent states with fixed quantum numbers equals to the dimensionality of the space, i.e., the dimension of the matrix (30),

$$\sum_P S_\ell^{(\mathrm{new})}(P) = \sum_P \langle\varphi_\ell^{(P)}|\hat{\mathcal{N}}_\ell^{-1}|\varphi_\ell^{(P)}\rangle = \sum_n 1. \quad (36)$$

In the case with one doorway configuration where, for example, the model space limits the number of four-nucleon operators (3) to just one for a fixed number of oscillator quanta n and partial wave ℓ, the single diagonal matrix element for the norm (32) can be expressed as

$$\langle\phi_{n\ell}|\hat{\mathcal{N}}_\ell|\phi_{n\ell}\rangle = \sum_P \mathcal{S}_\ell^{(\mathrm{old})}(P)\,, \quad (37)$$

therefore

$$S_\ell^{(\mathrm{new})}(P) = \frac{\mathcal{S}_\ell^{(\mathrm{old})}(P)}{\sum_{P'}\mathcal{S}_\ell^{(\mathrm{old})}(P')} = \frac{(\mathcal{F}_{n\ell}^{(P)})^2}{\sum_{P'}(\mathcal{F}_{n\ell}^{(P')})^2}. \quad (38)$$

The obtained sum rule represents an important property of the new spectroscopic factors. In contrast to the traditional definition they establish the total spectroscopic strength which is given by the number of possible doorway states identified by the value of the principle quantum number that the relative cluster-daughter nucleus motion can have assuming a fixed relative angular momentum ℓ. The presented sum rule provides grounds for qualitative conclusions about the distribution of clustering strength.

III. APPLICATIONS

α-clustering in sd-shell nuclei

The physics of sd-shell nuclei is one of the best examples demonstrating the success of the phenomenological shell model [56]. Therefore this mass region has been an appealing arena for testing and development of theoretical methods targeting nuclear clustering [24, 25, 28, 57, 58].

Experimentally the alpha clustering in low-lying states of sd-shell nuclei has been studied using transfer and knock-out reactions, such as the ones discussed in Refs. [59–62]. Some representative results for α-particle SFs for ground state to ground state transitions from previous experimental and theoretical works are shown in Tab. I. The experimental information is summarized in columns 2, 3, and 4 of Tab. I. Columns 2 and 3, from Refs. [63] and [64], respectively, show absolute values of SF's from knock-out reactions. Transfer reactions usually determine only relative values of the SFs, therefore the SFs presented in column 4 are normalized to the value of the SF in ^{20}Ne. Given that the experimental absolute value of SF in ^{20}Ne according to [63] is very close to 1.0, the remaining relative SFs in column 4 may be viewed as the absolute ones. The experimental data is subject to some substantial uncertainty coming from reaction models. In particular, the imaginary part of the nucleus-nucleus potential for the types of reactions involved is poorly known. Nevertheless, all experiments describe the variation of the relative values of the SFs with the increase in the nuclear mass consistently.

Similar theoretical results were obtained by various authors [24, 25] in the past. A set of representative theoretical SFs obtained by Chung et al., Ref. [24], is shown in Tab. I, column 5. Comparison of the previous theoretical values with the experimental data highlights some long-standing problems. First, the theoretical SFs are several times, and in certain cases nearly by an order of magnitude, smaller than the measured ones. In analogy with the approach taken in experiments involving transfer reactions, it is a common practice to renormalize theoretical data using the value of the α-particle SF in ^{20}Ne; and yet this leaves the question about the absolute scale unanswered. Second, even after renormalization the tendency for the theoretical values of SFs to decrease rapidly, while going from ^{20}Ne to ^{40}Ca, is not confirmed by the experimental data.

Our results for α-particle SFs for ground state to ground state transitions are listed in the 6th and 7th

$A_P - A_D$	$S_0^{(\mathrm{exp})}$ [63]	$S_0^{(\mathrm{exp})}$ [64]	$S_0^{(\mathrm{exp})}$ [65]	$\mathcal{S}_0^{(\mathrm{old})}$ [24]	$\mathcal{S}_0^{(\mathrm{old})}$ this work	$S_0^{(\mathrm{new})}$ this work
^{20}Ne-^{16}O	1.0	0.54	1	0.18	0.173	0.755
^{22}Ne-^{18}O			0.37	0.099	0.085	0.481
^{24}Mg-^{20}Ne	0.76	0.42	0.66	0.11	0.091	0.411
^{26}Mg-^{22}Ne			0.20	0.077	0.068	0.439
^{28}Si-^{24}Mg	0.37	0.20	0.33	0.076	0.080	0.526
^{30}Si-^{26}Mg			0.55	0.067	0.061	0.555
^{32}S-^{28}Si	1.05	0.55	0.45	0.090	0.082	0.911
^{34}S-^{30}Si				0.065	0.062	0.974
^{36}Ar-^{32}S				0.070	0.061	0.986
^{38}Ar-^{34}S			1.30	0.034	0.030	0.997
^{40}Ca-^{36}Ar	1.56	0.86	1.18	0.043	0.037	1

TABLE I: Ground state to ground state α-particle SFs: the experimental SFs $S_0^{(\mathrm{exp})}$ extracted from the cross sections of (p,pα) [63, 64] and (^{6}Li,d) [65] reactions, traditional $\mathcal{S}_0^{(\mathrm{old})}$ obtained in Ref. [24] and in the current work, and "new" SFs $S_0^{(\mathrm{new})}$.

columns of Tab. I. The calculations were performed using the USDB [56] Hamiltonian. The valence space is restricted by *sd*-shell. Within this model only one four-nucleon operator with SU(3) quantum numbers (8,0) contributes, and therefore the relationship (38) holds.

Our results, shown in the last (7th) column in Tab. I highlight the merits of the method and appear to resolve the above mentioned long-standing theoretical problems. Indeed, the agreement between absolute SFs found in experiment (columns 2–4) and those from our study (column 7) is good without any renormalizations. This includes the trend of SFs to drop down towards the middle of the *sd*-shell and to increase at the edges.

The traditional (old) SFs obtained by us are shown in Tab. I, column 6. Our results are close to the ones presented in Ref. [24] (column 5); the difference between the two does not exceed 20 percent. This emphasizes that the renormalization of the channel WFs proposed by Fliessbach, Eq. (28), is the main reason for this improvement.

α-clustering in ^{16}O

In this section we demonstrate the CNCIM in its full scale using the ^{16}O example. The structure of this nucleus is well studied experimentally. Multiple experimental methods with different probes have been used, leading to a wealth of information on single particle, collective, clustering and other properties. Over a hundred of excited states are known [66, 67], most of which are in the region between 10 and 20 MeV of excitation energy. This doubly-magic nucleus has been used as a challenge and a gauge for nuclear structure theories. As discussed in the introduction, the approach that we put forward appears to be most promising for providing a unified theoretical understanding of all experimentally available information. In our study we examine α-clustering of the ground and multiple excited states in ^{16}O relative to channels involving ^{12}C nucleus in the ground state. Both parent and daughter systems are treated in the unrestricted *p-sd* configuration space with effective interaction Hamiltonian from [34]. The study in Ref. [34] suggests that this effective Hamiltonian describes well the multi-particle correlations in ^{16}O which makes it a good choice for exploring clustering.

In order to obtain the wave functions in the factorized form (8) the spurious components are projected out using Glockner-Lawson procedure where the shell model Hamiltonian was diagonalized with the c.m. Hamiltonian ($H_{\mathrm{c.m.}} - {}^3/_2\hbar\omega$) scaled by a factor $\beta = 30\,\mathrm{MeV}/\hbar\omega$. The *p-sd* configuration space does not fully contain all c.m. excitatons, therefore the non-spurious states described by Eq. (8) with $0\hbar\omega$ c.m. excitation no longer form the null space of the ($H_{\mathrm{c.m.}} - {}^3/_2\hbar\omega$) Hamiltonian matrix exactly; this makes their exact projection impossible. However, it is well known empirically that the Glockner-Lawson approach is still very effective because the eigenvalues of ($H_{\mathrm{c.m.}} - {}^3/_2\hbar\omega$) matrix for non-spurious states in the truncated space are usually many orders of magnitude smaller than those of spurious states, and thus contamination with spurious components is small. In our study the largest contamination $\langle\Psi_P|\beta(H_{\mathrm{c.m.}} - {}^3/_2\hbar\omega)|\Psi_P\rangle \approx 0.3$ MeV was observed for the lowest 1^- state in ^{16}O. We estimate that the uncertainty in $S_\ell^{(\mathrm{new})}$ due to c.m. problem is about 0.005. Overall, in our study the c.m. problem appears to be insignificant when compared to other theoretical issues and uncertainties in experimental information.

The *p-sd* valence space allows for the following four-nucleon $|\Phi_{(n,0)} : \ell\rangle$ configurations:

$$|\Phi_{(n,0):\ell}\rangle = \big|(p)^q(sd)^{4-q}\,[4](n,0) : \ell, S{=}0, T{=}0\big\rangle, \quad (39)$$

where $q = 0, 1...4$; $n = 8 - q$; $\ell = n, n-2, ..., 1$ or 0; and $\pi = (-1)^\ell$.

A broad part of the low-lying ^{16}O spectrum was examined in our studies targeting the distribution of the alpha-cluster spectroscopic strength. We start with an overview of our results. In Fig. 1 the experimentally observed and theoretically calculated spectra of ^{16}O are presented, the scale is limited to about 17 MeV of excitation and only the states of natural parity are shown. The spectroscopic factors $S_0^{(\mathrm{new})}$, Eq.(34), are shown on the right, using the same energy scale. The distribution of the alpha spectroscopic factors appears to strongly support the clustering nature of the low-lying states found in other models; see [68, 69] and references therein.

The states $0_2^+, 2_1^+, 4_1^+$, and 6_2^+ are often viewed as the $K = 0$ rotational band [68, 70]. These states are highlighted in the figure. The B(E2) transitions involving these states are shown with arrows whose widths represent the strengths of the transitions. These reduced transition strengths are also listed in Tab. II and support the rotational nature of the band. For example, assuming $K = 0$ band and using the computed quadrupole moment of the first 2_1^+ state, $Q(2_1^+) = -12.5\,e\,\mathrm{fm}^2$,

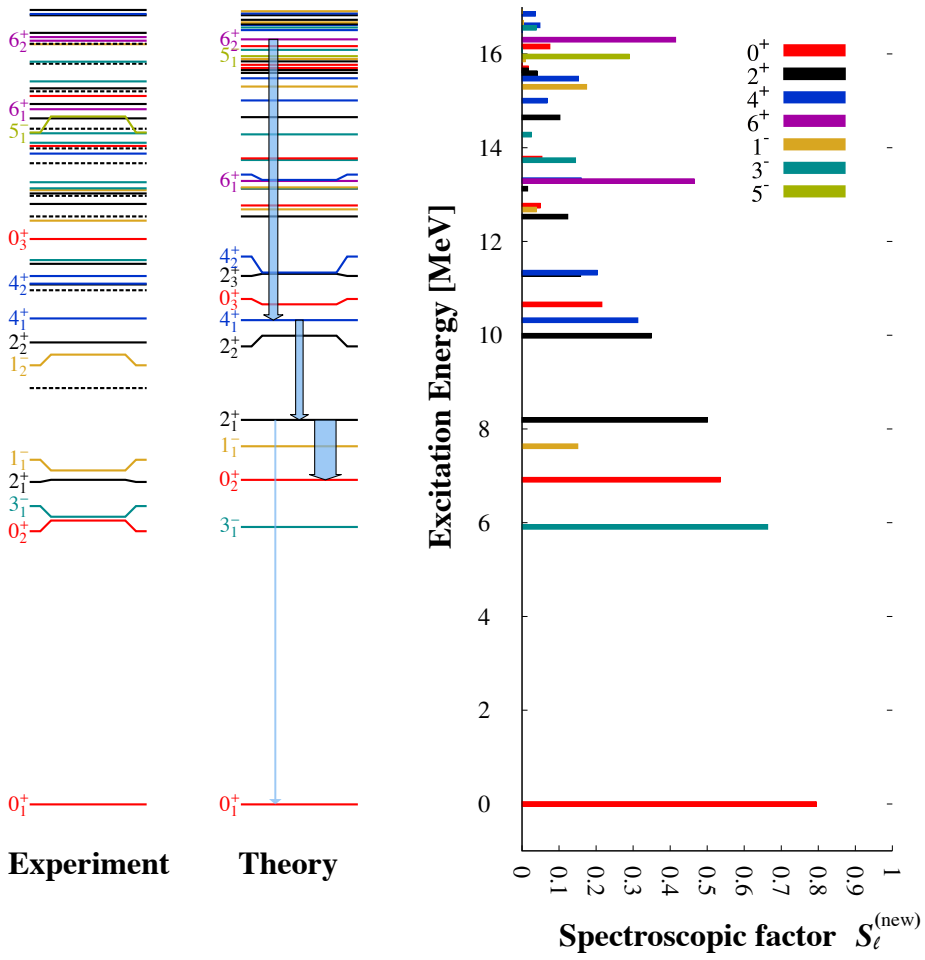

FIG. 1: (Color online) Spectrum of ^{16}O is shown: experimentally observed spectrum is on the left and calculated shell model spectrum is in the middle. Selected states are labeled with spin, parity, and with a number in subscript indicating their position ordered by excitation energy. On the right side, using the same vertical excitation energy scale, the distribution of spectroscopic factors $S_\ell^{(\mathrm{new})}$ is shown. The SFs are given for channels involving α and the ground state of ^{12}C, different colors are used to differentiate spins and parities.

the intrinsic quadrupole moment is found to be $Q_0 = -(7/2)Q(2_1^+) = 43.8\,e\,\mathrm{fm}^2$. For this intrinsic deformation $\mathrm{B(E2}, 2^+ \rightarrow 0^+) = Q_0^2/(16\pi) = 38.2\,e^2\,\mathrm{fm}^4$ agrees well with the value of $\mathrm{B(E2}, 2_1^+ \rightarrow 0_2^+)$ in Tab. II.

The detailed analysis of our results is summarized in Tab. III. The table is organized based on the theoretically calculated spectrum of ^{16}O. The first column identifies the spin, parity and the order in excitation energy of a state, the computed excitation energies and α-spectroscopic factors are listed in the second and third columns, respectively. We made an effort to identify each theoretically predicted state with an experimentally known counterpart. The table includes states of natural parity and zero isospin up to 22 MeV in excitation energy. In particular, the $T = 1$ states that are not listed in the table are $0^+_{7,10}$, $1^-_{3,7,12}$, $2^+_{9,10,14}$, $3^-_{2,8}$, $4^+_{6,9,13}$, and 5^-_5. Beyond 22 MeV the density of states is too high and only a very small fraction of states are identified experimentally. As a general rule, the states with spins $J = 4, 5$ are included up to 20 MeV of excitation, and those with $J \leq 3$ up to 18 MeV of excitation energy.

transition	B(E2)
$2_1^+ \rightarrow 0_1^+$	4.1
$2_1^+ \rightarrow 0_2^+$	44.2
$4_1^+ \rightarrow 2_1^+$	15.4
$4_1^+ \rightarrow 2_2^+$	4.2
$6_1^+ \rightarrow 4_1^+$	0.2
$6_2^+ \rightarrow 4_1^+$	18.3
$8_1^+ \rightarrow 6_1^+$	0.1
$8_1^+ \rightarrow 6_2^+$	31.7

TABLE II: List of selected B(E2) transitions computed for ^{16}O; the values are in units of $e^2\mathrm{fm}^4$. $\hbar\omega = 41\,A^{-1/3}$ MeV with $A = 16$ is assumed.

J_i^π	$E^{(\mathrm{sm})}$	$S_\ell^{(\mathrm{new})}$	$E^{(\mathrm{exp})}$	θ_α^2
0_1^+	0.000	0.794	0	0.86[a]
3_1^-	5.912	0.663	6.13	0.41[a]
0_2^+	6.916	0.535	6.049	0.40[a]
1_1^-	7.632	0.150	7.117	0.14
2_1^+	8.194	0.500	6.917	0.47[a]
1^-	no		9.585	0.67
2_2^+	9.988	0.349	9.844	0.0015
4_1^+	10.320	0.313	10.356	0.44
0_3^+	10.657	0.216	11.26	0.77
2_3^+	11.307	0.158	11.52	0.033
4_2^+	11.334	0.203	11.097	0.0014
3^-	no		11.6	0.68
2_4^+	12.530	0.123	no	
1_2^-	12.681	0.038	12.44	0.023
0_4^+	12.764	0.049	12.049	0.00036
2_5^+	13.125	0.015	13.02	<0.04
6_1^+	13.286	0.465	14.815	0.17
4_3^+	13.308	0.160	14.62	0.19
3_3^-	13.733	0.144	14.1	0.21
0_5^+	13.767	0.054	14.032	0.037
3_4^-	14.279	0.025	13.129	0.041
2_6^+	14.646	0.102	14.926	<0.0098
4_4^+	15.002	0.067	13.869	0.043
1_4^-	15.298	0.174	16.2	<0.085
1_5^-	15.884	0.009		
4_5^+	15.474	0.152	16.844	0.13
4_7^+	16.611	0.048		
4_8^+	16.855	0.036		
2_7^+	15.589	0.040	15.26	<0.052
2_8^+	15.649	0.016	16.352	<0.093

J_i^π	$E^{(\mathrm{sm})}$	$S_\ell^{(\mathrm{new})}$	$E^{(\mathrm{exp})}$	θ_α^2
0_6^+	15.694	0.017	15.097	<0.024
5_1^-	15.945	0.289	14.66	0.55
3_5^-	16.080	0.00063	15.408	<0.028
0_8^+	16.159	0.075	no	
6_2^+	16.304	0.415	16.275	0.43
3_6^-	16.557	0.038	15.828	0.14
2_{11}^+	16.720	0.011	16.93	<0.04
2_{12}^+	16.818	0.0096	17.129	<0.015
2_{13}^+	17.259	0.0032	17.197	<0.022
1_8^-	17.357	0.015	17.51	0.022
1_9^-	17.572	0.007		
1_{10}^-	17.674	0.016		
1_{11}^-	18.122	0.014		
3_9^-	17.772	0.034	no	
0_{11}^+	18.214	0.040	18.089	<0.033
4_{10}^+	18.251	0.051	17.784	<0.077
5_2^-	18.265	0.051	18.404	0.14
4_{11}^+	18.393	0.0079	18.016	0.0026
7_1^-	18.412	0.325	20.857	0.44
6_3^+	18.613	0.048	17.555	<0.11
4_{12}^+	19.081	0.030	18.785	<0.044
5_3^-	19.102	0.024	18.6	0.036
6_4^+	19.228	0.013	19.319	<0.023
4_{14}^+	19.348	0.015	19.375	<0.0036
4_{16}^+	19.819	0.028		
5_4^-	19.620	0.083	19.253	<0.011
8_1^+	20.018	0.34	no	
6_5^+	20.078	0.035	21.052	0.051
6_6^+	21.038	0.038	21.648	<0.026
7_2^-	21.693	0.036	21.623	<0.024

TABLE III: Shell-model ($E^{(\mathrm{sm})}$) and experimental ($E^{(\mathrm{exp})}$) energy levels, the α-particle SFs $S_\ell^{(\mathrm{new})}$ and the reduced widths θ_α^2 for states in ^{16}O. Symbol < denotes cases where only the total decay width is known.
[a] Recalculated values of the SFs from [71] (see the text).

The ^{16}O nucleus has proton and neutron separation energies at around 12.13 MeV and 15.6 MeV, respectively; therefore low-spin states above these energies have large single-nucleon decay widths. Focusing on the clustering properties in Tab. III, we restrict our presentation to the states with SFs greater than 0.005. Experimentally observed excitation energy $S_\ell^{(\mathrm{new})}$ and α spectroscopic strength θ_α^2 are listed in the last two columns. Most of the experimental information is taken from the spectroscopic tables [66, 67]. The reduced widths θ_α^2 of α decay were calculated using standard relations of resonance reaction theory. The values of θ_α^2 are viewed as the experimental SFs $S^{(\mathrm{new})}$, but it should be noted that the accuracy of this interpretation is limited. On the other hand, the values of θ_α^2 vary a lot from state to state, which makes its interpretation easier. For sub-threshold states the SFs are obtained using the (^{6}Li,d) reaction [71], those SFs are measured relative to 4_1^+ 10.356 MeV. Therefore some error is introduced by the rescaling of this data using the reduced width of the over-threshold reference state.

In establishing theory-experiment correspondence in Tab. III an agreement within a factor of 4 in SF is the primary criterion, a theory-experiment agreement in excitation energy within about 1 MeV is considered secondary.

Overall, we find the agreement between theory and experiment displayed in Tab. III encouraging; about $^2/_3$ of theoretical results obtained without introducing any parameters or fitting procedures turn out to be supported by the experimental data. For most levels observed in experiments theoretical partners may be found. Other properties of the ^{16}O states, such as electric quadrupole transitions and possible rotational bands, see Tab. II, are also well-described.

Discrepancies between theory and observations in Tab. III shed new light on the nature of states and provide guidance for further development of microscopic approaches to nuclear clustering and for future experiments.

First, for several states or groups of close-lying states predicted by theory, such as $1^-_{4,5}$, $4^+_{5,7,8}$, 0^+_8, $1^-_{8\ldots11}$, 3^-_9, $4^+_{14\ldots16}$, and 8^+_1, there are not enough equivalent states observed in experiments. It is likely that some states have been missed in experimental studies. Factors like high density of states, weak alpha decay branch, short lifetime of broad states can all prevent states from being observed.

Second, the most serious discrepancy that pertains to problems with theory is the absence of strongly clustered α-decaying states 1^- with $E^{(\mathrm{exp})}$=9.585 MeV and 3^- with $E^{(\mathrm{exp})}$=11.6 MeV. However, there is good evidence that these states correspond to configurations involving fp shell. In fact recent detailed experimental studies of ^{18}O show similar discrepancy, indicating that fp shell is needed for describing the strongly clustered 1^- and 3^- states [6].

Finally, there are some discrepancies in the distribution of strength, which is most noticeable in states 2_3^+ and 4_2^+. For the lowest four 4^+ states in the region between 10 and 15 MeV of excitation, the cumulative experimental and theoretical strengths, $\sum_i S_4^{(\mathrm{exp})}(4_i^+) = 0.67$ and $\sum_i S_4^{(\mathrm{new})}(4_i^+) = 0.74$, respectively, are in agreement. The situation is not as good with the 2^+ states where the cumulative measured strength $\sum_i S_2^{(\mathrm{exp})}(2_i^+) = 0.5$, which is less than a half of what is predicted by theory $\sum_i S_2^{(\mathrm{new})}(2_i^+) = 1.2$.

Overall, we find the agreement between theory and experiment displayed in Tab. III to be encouraging. The model includes no additional parameters, nor fits, and yet for most levels observed in experiments, theoretical partners may be found and acceptable level of agreement concerning alpha transition strength to ground state of ^{12}C is seen. Many states of a different nature with lower α SF, including those of non-zero isospin (not listed in Tab. III), are also reproduced by this theory. Other properties of the ^{16}O states that include electric quadrupole transitions and proton and neutron decay widths are also described by this model. The same approach can be applied to studies of the alpha-decay widths to excited states of ^{12}C. For example, the next channel of interest involves $\ell = 0$ and ^{12}C in the first excited 2_1^+ state which in our model is at 4.894 MeV of excitation. This channel is most strongly coupled to 2_2^+, 2_1^+, 2_3^+, 2_5^+, and 2_8^+ states of ^{16}O; the corresponding SF ($S_0^{(\mathrm{new})}$) are 0.32, 0.21, 0.17, 0.11, and 0.10, respectively. Unfortunately, experimental information about alpha decay in inelastic channels is very limited.

IV. SUMMARY

In this work we develop a formalism and methods for conducting studies of nuclear clustering using the advanced large-scale shell model technique. The formalism extends the configuration interaction technique, the modern shell model, towards clustering. Large configuration-space studies, interplay between cluster and nucleon degrees of freedom, cluster strength distribution at high excitation energies are the highlights of this technique. Numerous opportunities for extension and development make the approach promising.

We put forward a renormalization scheme which follows the Orthogonality Condition Model. We formally justify that the renormalizations are necessary for taking the Pauli exclusion principle into account and for constructing the wave functions of the cluster channels properly. The previously missing absolute normalization of the clustering strength emerges naturally from the developed formalism. We give a rigorous proof that the reformulated clustering strengths satisfy sum rules that are consistent with statistical properties of nuclear reactions.

We exemplify our approach by examining alpha cluster transitional spectroscopic strength between ground states of *sd*-shell nuclei. Our results implementing old techniques agree with previous theoretical studies that suffer from the long-standing problems related to underestimation of SFs and incorrectly predicted tendency of SFs to decrease with increasing nuclear mass. Renormalized new SFs are free of these issues and show good agreement with experiment.

We demonstrate our method by studying the ^{16}O nucleus. This nucleus is well studied experimentally, which makes it an ideal choice for the first application of our method. The study is done using an unrestricted *p*-*sd* valence space; over 60 exited states have been examined, and most of them are in agreement with experiment. The observables examined include excitation energies, alpha decay widths, as well as the traditional single-particle and electromagnetic properties. Our CNCIM approach has been successful in other recent experimental studies of ^{18}O in Ref. [6].

Acknowledgments

We thank T. Dytrych, V. Goldberg, and G. Rogachev for motivating discussions. This material is based upon work supported by the U.S. Department of Energy Office of Science, Office of Nuclear Physics under Award Number DE-SC-0009883.

[1] C. Beck, *Clusters in nuclei*, vol. 818,848,875 (Springer, Berlin ; New York, 2010).
[2] K. Artemov and et al., Sov. J. Nucl. Phys. **52**, 406 (1990).
[3] V. Goldberg and A. Pakhomov, Phys. At. Nucl. **56**, 1167 (1993).
[4] T. Lönnroth, M. Norrby, V. Goldberg, G. Rogachev, M. Golovkov, K. M. Källman, M. Lattuada, S. Perov, S. Romano, B. Skorodumov, et al., Eur. Phys. J. A **46**, 5 (2010).
[5] M. Norrby, T. Lönnroth, V. Z. Goldberg, G. V. Rogachev, M. S. Golovkov, K. M. Källman, M. Lattuada, S. V. Perov, S. Romano, B. B. Skorodumov, et al., Eur. Phys. J. A **47**, 73 (2011).
[6] M. L. Avila, G. V. Rogachev, V. Z. Goldberg, E. D.

Johnson, K. W. Kemper, Yu. M. Tchuvil'sky, and A. S. Volya, Phys. Rev. C **90**, 024327 (2014).
[7] I. A. Gnilozub, S. D. Kurgalin, and Yu. M. Tchuvl'sky, J. Phys.: Conf. Ser. **436**, 012034 (2013).
[8] Y. Kanada-En'yo and H. Horiuchi, Prog. Theor. Phys. Supp. **142**, 205 (2001).
[9] T. Neff and H. Feldmeier, Int. J. Mod. Phys. E **17**, 2005 (2008).
[10] S. C. Pieper, R. B. Wiringa, and J. Carlson, Phys. Rev. C **70**, 054325 (2004).
[11] P. Navratil and S. Quaglioni, Phys. Rev. Lett. **108**, 042503 (2012).
[12] E. Caurier, G. Martinez-Pinedo, F. Nowacki, A. Poves, and A. P. Zuker, Rev. Mod. Phys. **77**, 427 (2005).
[13] I. Talmi, *Fifty years of the nuclear shell model-the quest for the effective interaction*, vol. 27 of *Advances in Nuclear Physics* (Kluwer Academic Publishers, 2003).
[14] B. A. Brown, Prog. Part. Nucl. Phys. **47**, 517 (2001).
[15] A. Volya, Phys. Rev. C **79**, 044308 (2009).
[16] A. Volya and V. Zelevinsky, Phys. Rev. Lett. **94**, 052501 (2005).
[17] B. R. Barrett, P. Navratil, and J. P. Vary, Prog. Part. Nucl. Phys. **69**, 131 (2013).
[18] K. Varga, R. G. Lovas, and R. J. Liotta, Nucl. Phys. **A550** (1992).
[19] K. Varga and R. J. Liotta, Phys. Rev. C **50**, R1292 (1994).
[20] A. Insolia, P. Curutchet, R. J. Liotta, and D. S. Delion, Phys. Rev. C **44**, 545 (1991).
[21] S. G. Kadmensky, S. D. Kurgalin, and Yu. M. Tchuvil'sky, Phys. Part. Nucl. **38**, 699 (2007).
[22] H. J. Mang, Z. Phys. **148**, 582 (1957).
[23] Yu. F. Smirnov and Yu. M. Tchuvil'sky, Phys. Rev. C **15**, 84 (1977).
[24] W. Chung, J. van Hienen, B. H. Wildenthal, and C. L. Bennett, Phys. Lett. B **79**, 381 (1978).
[25] M. Grigorescu, B. A. Brown, and O. Dumitrescu, Phys. Rev. C **47**, 2666 (1993).
[26] Yu. M. Tchuvil'sky, W. W. Kurowsky, A. A. Sakharuk, and V. G. Neudatchin, Phys. Rev. C **51**, 784 (1995).
[27] P. Navratil, Phys. Rev. C **70**, 054324 and 014317 (2004).
[28] M. Ichimura, A. Arima, E. C. Halbert, and T. Terasawa, Nucl. Phys. A **204**, 225 (1973).
[29] O. F. Nemetz, V. G. Neudatchin, A. T. Rudchik, Yu. F. Smirnov, and Yu. M. Tchuvil'sky, *Nucleon Clusters in Atomic Nuclei and Multi-Nucleon Transfer Reactions* (Naukova Dumka, Kiev, 1988), p. 295.
[30] M. Norrby, T. Lönnroth, V. Z. Goldberg, G. V. Rogachev, M. S. Golovkov, K. M. Källman, M. Lattuada, S. V. Perov, S. Romano, B. B. Skorodumov, et al., Eur. Phys. J. A **47**, 96 (2011).
[31] T. Fliessbach and H. Mang, Nucl. Phys. A **263**, 75 (1976).
[32] R. G. Lovas, R. J. Liotta, A. Insolia, K. Varga, and D. S. Delion, Phys. Rep. **294** (1998).
[33] R. Id Betan and W. Nazarewicz, Phys. Rev. C **86**, 034338 (2012).
[34] Y. Utsuno and S. Chiba, Phys. Rev. C **83**, 021301 (2011).
[35] *Nuclear theory in the supercomputing era – 2013* (2014), http://ntse-2013.khb.ru/proceedings/, eds. A. M. Shirokov and A. I. Mazur.
[36] A. Volya and Yu. M. Tchuvil'sky, *Study of Nuclear Clustering Using the Modern Shell Model Approach* (World Scientific, 2014), p. 215, Exotic Nuclei, IASEN-2013, ISBN 978-981-4632-03-4, eds. E.Cherepanov, Yu. Penionzhkevich, D. Kamanin, R. Bark and J. Cornell.
[37] A. Volya and Yu. M. Tchuvil'sky, J. Phys.: Conf. Ser. **569**, 012054 (2014).
[38] Yu. M. Tchuvil'sky and A. Volya, JPS Conf. Proc. (2014), in press.
[39] Yu. M. Tchuvil'sky and A. Volya, *Nuclear Theory in the Supercomputing Era — 2014(NTSE-2014)* (2014), URL `http://ntse-2014.khb.ru/proceedings/`.
[40] R. D. Lawson, *Theory of the nuclear shell model* (Clarendon Press, Oxford, 1980), ISBN 0198515162.
[41] I. V. Kurdyumov, Yu. F. Smirnov, K. V. Shitikova, and S. Kh. El Samarai, Nucl. Phys. A **145**, 593 (1970).
[42] Yu. F. Smirnov, Nucl. Phys. **27**, 177 (1961).
[43] D. Sääf and C. Forssén, Phys. Rev. C **89**, 011303 (2014).
[44] D. Gloeckner and R. Lawson, Phys. Lett. B **53**, 313 (1974).
[45] I. Talmi, Helv. Phys. Acta **25**, 185 (1952).
[46] M. Moshinsky, Nucl. Phys. **13**, 104 (1959).
[47] Yu. F. Smirnov, Nucl. Phys. **39**, 346 (1962).
[48] L. Trlifaj, Phys. Rev. C **5**, 1534 (1972).
[49] B. Buck and A. Merchant, Nucl. Phys. A **600**, 387 (1996).
[50] Yu. F. Smirnov and Yu. M. Tchuvil'sky, Czech. J. Phys. **33**, 1215 (1983).
[51] S. Saito, Prog. Theor. Phys. **41**, 705 (1969).
[52] T. Fliessbach and P. Manakos, J. Phys. G **3**, 643 (1977).
[53] P. Descouvemont and M. Dufour, *Clusters in Nuclei, Vol 2* (2012), vol. 848 of *Lecture Notes in Physics*, p. 1, ISBN 978-3-642-24707-1.
[54] S. Quaglioni and P. Navratil, Phys. Rev. C **79**, 044606 (2009).
[55] S. Yu. Igashov and Yu. M. Tchuvil'sky, Eur. Phys. J. Web Conf. **38**, 16002 (2012).
[56] B. A. Brown and W. A. Richter, Phys. Rev. C **74**, 034315 (2006).
[57] J. P. Draayer, Nucl. Phys. A **237**, 157 (1975).
[58] K. T. Hecht and D. Braunschweig, Nucl. Phys. A **244**, 365 (1975).
[59] W. Oelert, W. Chung, A. Djaloeis, C. Mayer-Böricke, and P. Turek, Phys. Rev. C **22**, 408 (1980).
[60] W. Oelert, W. Chung, M. Betigeri, A. Djaloeis, C. Mayer-Böricke, and P. Turek, Phys. Rev. C **20**, 459 (1979).
[61] H. W. Fulbright, Ann. Rev. Nucl. Part. Sci. **29**, 161 (1979).
[62] N. Anantaraman, H. W. Fulbright, and P. M. Stwertka, Phys. Rev. C **22**, 501 (1980).
[63] T. Carey, P. Roos, N. Chant, A. Nadasen, and H. L. Chen, Phys. Rev. C **23**, 576(R) (1981).
[64] T. Carey, P. Roos, N. Chant, A. Nadasen, and H. L. Chen, Phys. Rev. C **29**, 1273 (1984).
[65] N. Anantaraman and et al., Phys. Rev. Lett. **35**, 1131 (1975).
[66] D. R. Tilley, H. R. Weller, and C. M. Cheves, Nucl. Phys. A **564**, 1 (1993).
[67] *Evaluated nuclear structure data file*, URL `http://www.nndc.bnl.gov/ensdf/`.
[68] M. Freer, Rep. Prog. Phys. **70**, 2149 (2007).
[69] T. Yamada and et al., *Clusters in Nuclei, Vol 2* (2012), vol. 848 of *Lecture Notes in Physics*, p. 229, ISBN 0075-8450.
[70] W. Bauhoff, H. Schultheis, and R. Schultheis, Phys. Rev. C **29**, 1046 (1984).
[71] F. D. Becchetti, D. Overway, J. Jänecke, and W. W. Jacobs, Nucl. Phys. A **344**, 336 (1980).